

## Interfacial instability and DNA fork reversal by repair proteins

This article has been downloaded from IOPscience. Please scroll down to see the full text article.

2010 J. Phys.: Condens. Matter 22 155102

(<http://iopscience.iop.org/0953-8984/22/15/155102>)

[The Table of Contents](#) and [more related content](#) is available

### Download details:

IP Address: 203.129.207.10

The article was downloaded on 10/03/2010 at 04:28

Please note that [terms and conditions apply](#).

# Interfacial instability and DNA fork reversal by repair proteins

Somendra M Bhattacharjee

Institute of Physics, Bhubaneswar 751005, India

E-mail: [somen@iopb.res.in](mailto:somen@iopb.res.in)

Received 27 October 2009, in final form 7 January 2010

Published 9 March 2010

Online at [stacks.iop.org/JPhysCM/22/155102](http://stacks.iop.org/JPhysCM/22/155102)

## Abstract

A repair protein like RecG moves the stalled replication fork in the direction from the zipped to the unzipped state of DNA. It is proposed here that a softening of the zipped–unzipped interface at the fork results in the front propagating towards the unzipped side. In this scenario, an ordinary helicase destabilizes the zipped state locally near the interface and the fork propagates towards the zipped side. The softening of the interface can be produced by the aromatic interaction, predicted from the crystal structure, between RecG and the nascent broken base pairs at the Y-fork. A numerical analysis of the model also reveals the possibility of a stop and go type motion.

(Some figures in this article are in colour only in the electronic version)

## 1. Introduction

The semi-conservative replication of DNA requires that DNA be unzipped and new strands be synthesized over each of the opened parent strands. The unzipping is done by helicases while the synthesis is by dna-polymerases, e.g., by DNA polymerase III. The basic features of the replication process are as follows [1, 2]. The two strands of DNA run in opposite directions. The polymerase is highly specific with a unidirectional 3′-5′ motion on a DNA strand. As a result, a polymerase can follow the helicase only on one strand, but not on the other. The strand that offers an unhindered motion is called the *leading strand* while the other one in the opposite direction is the *lagging strand*. Although the two polymerases on the two strands are identical, the lagging strand polymerase performs a more complicated job. For synchronization with unzipping, it (i) makes the new strand in pieces (Okazaki fragments), (ii) shifts repeatedly to newer positions closer to the moving helicase, and (iii) restarts the polymerization process anew after every shift. To complete the cycle for a longer DNA strand, the small Okazaki fragments are joined by dna ligase. In addition, there are requirements of a primase for every initiation of the Okazaki fragments, of sliding clamp proteins to tether the polymerases to DNA, to name a few more. Even with this complexity, the replication process is known to be highly processive; in this context processivity is defined as the number of base pairs added at a stretch each time the replication machinery binds to DNA (for *E. Coli*, the

$4.6 \times 10^6$  base pair long DNA is ultimately replicated in 40mins with a rate constant  $\sim 10^{-3} \text{ s}^{-1}$  for helicase dissociation from DNA [3]). Moreover, the fidelity of replication requires additional repair or proof-reading capabilities which becomes functional as and when needed. It is known that most of the polymeric molecules of the replication machinery can work independently *in vitro*, but all of these do work in tandem over a long time and long distance (along the DNA) for the processivity observed during replication.

The controversy with replication dynamics can be summarized in the following way [1, 2]. In one class of models, the replication machineries move on the DNA. See figure 1(a). Here one needs a tight coupling between the lagging strand polymerase and the helicase to facilitate repeated recognition of the newly unzipped region of DNA. Not only these, but others such as the primase or the ligase, should get correlated on the lagging strand. The antithesis is the proposal of a replisome—a complex of all the objects staying together, with the DNA looping through the complex in a very particular manner [4]. See figure 1(b). Since the DNA goes through the replisome, there is expected to be a depletion region of nutrients surrounding a replisome, to be supplemented by a current towards it. More perplexing is, that if a complex can exist for a long enough time during replication, then why it is so elusive *in vitro* and what is responsible for the ‘bound state’ *in vivo*.

Different types of experiments in recent years explored the nature of the dynamics. Single molecular experiments

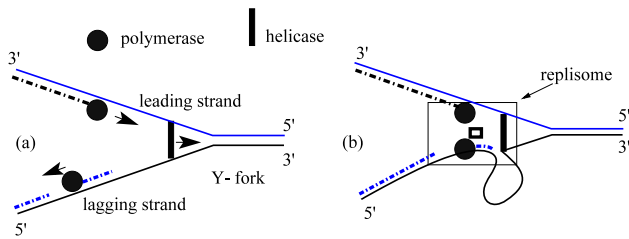


**Figure 1.** Schematic diagram of the replication process. Only the helicase and the polymerases are shown, with arrows indicating the directions of motion. The solid lines are the parent DNA strands with 3', 5' ends marked. The dash-dot lines represent the newly synthesized DNA. In (a), the members of the replication machinery move on the DNA individually. The small fragments on the lagging strand are the Okazaki fragments. The replisome model is shown in (b). The small thick lined box is the clamp loader that loads the lagging strand DNA on the replisome. In both models, the whole machinery works near the Y-fork.

revealed correlations between the synthesis by a T7 DNA polymerase and the T7 helicase activity on a dsDNA; an efficient duplex DNA synthesis requires the combined action of polymerase and helicase, but no direct or specific interaction between the polymerase and the helicase plays any role [5]. For bacteriophage T4, the assembly of the polymerase and the clamp loader with DNA has been found to be highly dynamic and well coordinated [6]. The 'replisome' may itself be dynamic in nature with not just two but even three polymerases, and others like repair factors can be dynamically attached to it [7]. The probability distributions of the lengths of the Okazaki fragments for T4 and T7 have been found to be very broad and highly non-Gaussian [8]. This is to be contrasted with the very sharp distributions expected from individual primase controlled models, or, if the replication process were tightly controlled, hard-coded in the functioning of the molecules. Purely stochastic models have been proposed to study correlations in Okazaki fragment distributions [9]. These newer experimental methods and analysis, apart from elucidating the nature of the complexity of replication, are also bringing out the importance of the dynamics and correlations (also called coordination) of the protein complexes and DNA strands, in particular near the fork.

An important aspect of the replication process is the repair mechanism also involving helicases. A helicase is a motor protein that generally facilitates in opening the DNA and leads the replication machineries. Such a helicase moves from the unzipped (i.e., the open side) to the zipped or bound side. There are actually many helicases, e.g. almost 20 in *E. Coli* (though it is not clear why there are so many), but, generically, all of them are known to have a piece that maintains the two strands of DNA at a distance much larger than the base pair distance. This piece is called the wedge domain. The motor action (e.g. for dnaB [10]) and often additional pulling action (e.g. PcrA [11]) carry out the opening process. The helicase activity stops in the case where there is a nick or a lesion on the leading strand. The replication process stalls, and the whole replication assembly disperses. At this juncture, a repair process takes over. Often, RecG is the helicase that starts the repair job by performing a fork reversal [12].

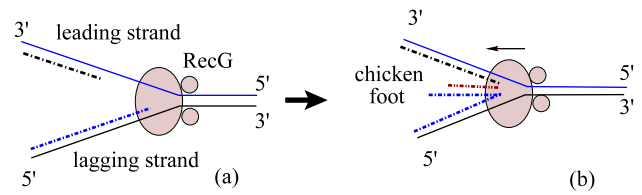


**Figure 2.** Schematic diagram of the repair process by RecG (shaded ellipse and two circles) at the Y-fork. (a) RecG at the stalled Y-fork with a longer lagging strand pair. (b) Fork reversal and chicken-foot configuration (Holliday junction). The arrow denotes the direction of motion of the fork. The four arm junction is created by the fork reversal and the continuation of the leading strand pair by making use of the pair on the lagging strand.

Taking a cue from the crystal structure, it is suggested that the wedge domain of RecG maintains the large separation of the DNA strands, but there are two other domains that sit on the zipped side to push the DNA towards the unzipped side. The end result is that the Y-fork moves towards the unzipped side and the DNA is scooped out on the lagging strand [13]. See figure 2. This process continues until the nascent end on the leading strand is reached. The structure formed is a chicken-foot configuration. The job of RecG is now over, the repair process is completed by other objects via a Holliday junction, and, then the replication restarts. In this model, RecG has two jobs, zipping the parent strands and unzipping the nascent duplex on the lagging strand. The activities of a pre-assembled RecG–DNA on (i) a three-way DNA (consisting of the Y-fork with a nascent duplex on the lagging strand) and (ii) a two-way DNA (consisting of a pure Y-fork) are found to be the same, if initial transients are ignored [14]. We therefore take the view that the main job in the repair process of RecG is the zipping of the DNA or the fork reversal.

Our purpose in this paper is to show how a coupling of the helicase and the replication fork (Y-fork) can be used to formulate the backward mobility of RecG-like repair proteins, in addition to the forward motion of general helicases. Our hypothesis is that the Y-fork is an essential element in the whole replication process, and it is at the heart of the correlated dynamics [15]. This hypothesis is based on the observations that in both the biological models and the experiments mentioned earlier, the common feature is the proximity of a Y-fork—the junction of an unzipped and a zipped DNA, and that dynamics plays an important role, to the extent that it may even be responsible for the formation of the replisome.

The first step to motivate this connection is to analyse the helicase activity. Traditionally, DNA opening is considered as a melting phenomenon, where thermal noise, fluctuations in base pair breaking–joining, and polymer configurations play important roles [1]. A different mechanism is the force induced unzipping transition at temperatures below the melting point [16–21]. In the unzipping scenario, since the unzipping transition is first order in nature, there can be a coexistence of the two phases separated by a domain wall. This phase coexistence of the zipped and unzipped phases with the domain wall is *the* Y-fork. With an applied force,

such a coexistence can happen only at a particular value of the force, but no such special condition is required in the fixed distance ensemble [19]. By definition, in the fixed distance ensemble, a particular base pair of DNA is kept at a fixed distance. The wedge domain of a helicase provides such a constraint to maintain the DNA in a fixed distance ensemble, and, therefore, a Y-fork develops. The helicase activity is then tantamount to setting the Y-fork interface in motion, the energy being supplied almost exclusively by ATP. Therefore, the Y-fork owes its origin to the equilibrium unzipping phase transition, but its real time dynamics or motion is, in general, a nonequilibrium phenomenon. In this language, the synchronization or coordination problem of replication can be recast as a velocity selection problem. The Y-fork dynamics is described by the internal dynamics of DNA, the helicase motion is controlled by the energy supply and its own dynamical mechanism, and similarly for other individuals. Thus, each has its own characteristic velocity when acting alone, and that is the velocity one measures *in vitro* [22]. In spite of this diversity, all of these should have the same velocity when acting together during replication. Hence, the issue of velocity selection. Similarly, a repair process is not just a resealing of the Y-fork under DNA dynamics but has to be closely knit with the repair process. This, too, requires velocity selection. The speciality of RecG is seen from the crystal structure, which indicates a competition of the closed rings of the wedge domain with the nascent broken pairs of the DNA through aromatic interaction [13, 12]. That both the forward and the backward motions can be handled in the same framework lends credence to the basic hypothesis.

The outline of the paper is as follows. Using a Landau type functional to describe the zipped—unzipped coexistence we formulate the propagating front equation when there is a local perturbation around the interface. The coupling of RecG with the interface is then introduced and the effective dynamics written down. The dynamics discussed is nonequilibrium, with the drive coming from the motion of the perturbation. The Landau free energy incorporates thermal fluctuations in a coarse-grained form. This is justified so long as one is not too close to the melting point of DNA ( $T_c \sim 80\text{--}100\text{C}$ ). For temperatures close to  $T_c$ , bubble formation along the zipped region of DNA would affect the overall motion of the helicase because of the sudden release of longer strands as the Y-fork hits a bubble. We avoid this strong fluctuation regime by staying far below the melting point, which is consistent with real physiological conditions (temperature  $T < T_c$ ). Section 2 discusses this formulation of dynamics. In the same section, we discuss the strong coupling limit of the RecG–Y-fork interaction that leads to an instability important for the fork reversal. In section 3, a perturbative approach is used to calculate, via a Goldstone mode, the velocity of propagation, the starting point being the zero velocity coexisting phase situation. A numerically exact solution of a discretized version of the model is then presented in Apart from the verification of the predictions of the perturbation theory, nonperturbative effects are also found. Section 4 is the summary and conclusion.

## 2. Model and velocity selection

### 2.1. Dynamics

We start with the fact that a double-stranded DNA in equilibrium below its melting point can show phase coexistence with an interface separating the two phases, the zipped and the unzipped phases. A helicase (or its wedge domain mentioned in section 1) provides the necessary constraint of a fixed distance ensemble to generate the coexistence. To open the DNA this interface needs to be translocated.

For standard helicases like dnaB, the motor action just forces through the DNA, so that as the location of the constraint of the fixed distance ensemble shifts, the bound state region becomes metastable or unstable with respect to the unzipped state. For helicases like PcrA, there is an additional pull by a hand like branch on the DNA strand near the Y-fork. This is also an example of an active mechanism to make the state near the Y-fork meta- or unstable but not in the bulk. With this in mind, let us formulate our model in the following way. The equilibrium phase coexistence—Y-fork—by a static helicase, can be described by a Landau like free energy  $F_h(\phi)$ , where  $\phi$  is a scaled distance. By choosing  $\phi = 0$  as the bound state and  $\phi = 1$  as the open state, with a slightly negative  $\phi$  representing an overtight state, we take

$$f_h(\phi) \equiv -\frac{dF_h(\phi)}{d\phi} = \phi\left(\phi - \frac{1}{2} + h\right)(1 - \phi), \quad (1)$$

so that the effective Landau–Hamiltonian can be written as

$$\mathcal{F}\{\phi\} = \int dz \left[ \frac{D}{2} \left( \frac{\partial\phi}{\partial z} \right)^2 + F_h(\phi) \right], \quad (2)$$

where  $D$  is an elastic constant and

$$F_h(\phi) = \frac{\phi^2}{4} - \frac{\phi^3}{2} + \frac{\phi^4}{4} + h \left( -\frac{\phi^2}{2} + \frac{\phi^3}{3} \right). \quad (3)$$

The phase coexistence occurs at  $h = 0$ . The coefficients are chosen, for simplicity, to have the extrema of  $F_h$  in a symmetrical fashion. The perturbation  $h > 0$  makes the unzipped state the favoured phase. See figure 3(a). The dynamics is described by

$$\frac{\partial\phi}{\partial t} = -\frac{\delta\mathcal{F}}{\delta\phi} = D \frac{\partial^2\phi}{\partial z^2} + f_h(\phi), \quad (4)$$

with the boundary condition:

$$\phi(-\infty) = 1, \quad \phi(+\infty) = 0, \quad (5)$$

and  $h(z, t)$  is non-zero only near the interface. In equations (1) and (4),  $f_h$ , represents the effective force. The boundary conditions ensure that we have an open or unzipped strand on the left side with a closed terminal on the right side. The chain length has been taken to be infinity. Despite the resemblance, this is not the Fisher–Kolmogorov problem [23, 24] because there is *no* bulk instability here.

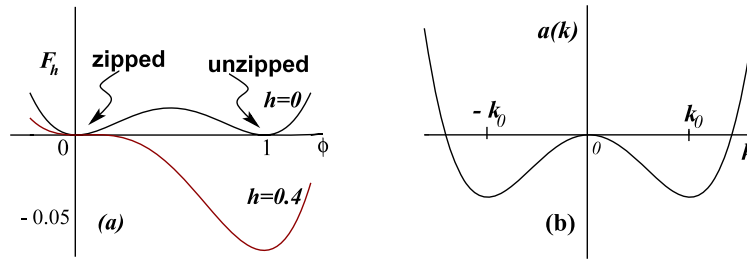


**Figure 3.** (a)  $F_h(\phi)$  versus  $\phi$  for  $h = 0$  and  $0.4$ . The perturbation by  $h$  makes the unbound state the stable phase. (b)  $a(k)$  versus  $k$  for the  $D' < 0$  case. The minima at  $k = \pm k_0$  suggest that the stable state is not the homogeneous state with  $\phi = 0$  or  $1$ , but a different state with a modulating wavevector  $k = k_0$ .

Where is the helicas in this set of equations? For the static case,  $h = 0$ , and there is no propagation. The boundary conditions impose a kink  $\phi(z)$  that goes from  $\phi = 1$  to  $0$ , but the location  $z_0$  of the kink is arbitrary [25]. This is a Goldstone like mode; the interface or the kink separating the unzipped and the zipped phases can be placed anywhere along the chain because neither equation (4) cares about  $z_0$ , nor there is any energy cost in shifting the interface. However, a static helicas fixes the position of the Y-fork and therefore it kills the Goldstone mode by fixing  $z_0$  where the Y-fork would be. The local instability is taken into account by  $h(z, t)$ , which parameterizes the motor action and the active mechanism of the helicas. In short, the helicas at time  $t = 0$  is replaced by two features: (i) the time independent boundary conditions and the location of the initial Y-fork represent the wedge domain, and (ii) the passive or active process of the helicas is represented by the local instability parameter  $h$ .

The dynamic activity of a helicas makes  $z_0$  a function of time. A propagating mode would imply

$$\phi(z, t) \equiv \Phi(z - ct), \quad (6)$$

with  $c$  the velocity of the front. The helicas must move with the same velocity and so must the perturbation. The drive for the nonequilibrium motion, supplied by ATP in reality, is modelled by the requirement that the perturbation  $h(z, t)$  moves with the interface. Therefore,

$$h(z, t) \equiv H((z - ct)/W), \quad H(z) \neq 0 \quad \text{for } |z| < 1. \quad (7)$$

This matching of velocity is the velocity selection mentioned earlier.  $W$  is the width of the region over which the helicas affects the fork. A simpler, more practical, choice would be an implicit definition  $h \neq 0$  for  $|\phi - \phi_h| \leq \delta\phi_w$ .

RecG is similar to other helicas as far as the existence of a wedge domain is concerned, but its interaction is with the broken bonds at the interface (more like a surfactant). In other words, unlike an ordinary helicas that unzips, it does not produce an instability of any phase but rather interacts with the interface. With that in mind we introduce a new Gaussian variable  $y(z, t)$  representing the helicas and its interaction with the interface (for which  $\partial\phi/\partial z \neq 0$ ) as

$$\mathcal{F}\{\phi\} = \int dz \left[ \frac{D}{2} \left( \frac{\partial\phi}{\partial z} \right)^2 + F_0(\phi) + 2\lambda y \frac{\partial\phi}{\partial z} + Ky^2 \right], \quad (8)$$

with ( $K > 0$ ), where the subscript 0 indicates  $h = 0$  in equation (1), i.e., there is no perturbation in the coexisting part of the free energy.

Instead of coupled dynamics, we consider the effective dynamics of the Y-fork by integrating out the  $y$  field. Such an integration leads to a new effective Hamiltonian of the same type as equation (2), with a reduced elastic constant  $D' = D - \lambda^2/K$ . For sufficiently large  $\lambda$ ,  $D'$  can become negative and for stability a higher-order term is added. The effective Landau energy can then be taken as

$$\mathcal{F}\{\phi\} = \int dz \left[ \frac{D'}{2} \left( \frac{\partial\phi}{\partial z} \right)^2 + \frac{\gamma}{2} \left( \frac{\partial^2\phi}{\partial z^2} \right)^2 + F_0(\phi) \right]. \quad (9)$$

The dynamics is given by

$$\frac{\partial\phi}{\partial t} = D \frac{\partial^2\phi}{\partial z^2} - \gamma \frac{\partial^4\phi}{\partial z^4} - h_R \frac{\partial^2\phi}{\partial z^2} + \phi \left( \phi - \frac{1}{2} \right) (1 - \phi), \quad (10)$$

where the helicas (perturbing) part is written explicitly as the  $h_R$  term, with  $h_R \neq 0$  in a region near  $\phi = 0$ . We use the fact that RecG operates near the zipped side. With negative  $D'$ , there is a preference for a modulated structure. To see the effect of  $D' < 0$ , we rewrite the gradient-dependent part of  $\mathcal{F}\{\phi\}$  in Fourier modes as

$$\mathcal{F}(\phi) = \frac{1}{2} \int dk a(k) \phi_k \phi_{-k}, \quad (11)$$

where

$$\phi(z) = \int \frac{dk}{(2\pi)^{1/2}} e^{ikz} \phi_k, \quad \text{and} \quad a(k) = D'k^2 + \gamma k^4.$$

This favours, as shown in figure 3(b), a modulated state with wavevector  $k_0 = \gamma/|D'|$ . Such a modulated structure would be a state with bubbles—but that does not happen here because the perturbation is only local, meant to destabilize the interface.

The difference between the two types of helicas is now seen in the respective  $h$ -type terms. In equation (4), the  $h$ -term affects the stability of the phase while in equation (10) it affects the interface.

### 3. Perturbative approach and numerical solution

We now treat the helicas effect as a small perturbation and show the change in the direction of velocity in the two cases

in a first-order perturbation theory. Let us take equation (2) for illustration. If there is no perturbation, then the free energy, equations (1) and (2), suggest a static interface, i.e., velocity  $c = 0$ . The profile with small perturbation can therefore be written as

$$\phi = \phi_0(z) + \delta\phi(z - ct, t), \quad (12)$$

where the zeroth-order solution is the static solution satisfying

$$D \frac{\partial^2 \phi_0}{\partial z^2} + \phi_0 \left( \phi_0 - \frac{1}{2} \right) (1 - \phi_0) = 0. \quad (13)$$

For the boundary conditions of equations (4), (13) gives the static kink solution  $\phi_0(z)$  that gives the  $z$ -dependent profile near the interface [25]. The perturbed part satisfies, to first order, an inhomogeneous differential equation

$$\left[ \frac{\partial}{\partial t} - D \frac{\partial^2}{\partial z^2} - f'(\phi_0) \right] \delta\phi = \delta f(\phi_0) = h\phi_0(1 - \phi_0), \quad (14)$$

where  $f'(\phi_0) = df/d\phi|_{\phi=\phi_0}$ . The solution of this equation can be written in terms of the Green function [24]

$$\delta\phi = \int_{t_0}^t d\tau \int_{-\infty}^{\infty} d\xi G(t, \tau, z, \xi) \delta f(\phi_0). \quad (15)$$

Moreover, to first order, the velocity  $c$  is small and the perturbed part can be written as

$$\delta\phi = \frac{d\phi_0}{dz} (t - t_0)c.$$

This shows that the velocity can be determined from the coefficient of the term linear in  $t$ .

The Green function has an eigenfunction expansion for the spatial part

$$\left[ D \frac{\partial^2}{\partial z^2} + f'(\phi_0) \right] \psi_n = E_n \psi_n, \quad (16)$$

where  $E_n$  are the eigenvalues and  $\psi_n$  the corresponding eigenfunctions. Since we are considering a dissipative system, it is guaranteed that  $E_n \geq 0$ . For all the eigenfunctions with  $E_n > 0$ , the Green function will have a time contribution  $G(t, t_1, z, z_1) \sim \exp(-E_n(t - t_1))$ , so that in the long time limit, these modes will not contribute, except for the initial transients.

The Goldstone mode corresponds to a solution with  $E_0 = 0$  as can be verified directly with  $\psi_0 = d\phi_0/dz$ . This zero mode produces a linear term in the solution (not an exponential decay in time) and the velocity of the front comes from this term only. The velocity is then given by

$$c = \frac{\int \phi'_0(z_1) (\delta f(z_1)) dz_1}{\int [\phi'_0(z_1)]^2 dz_1}. \quad (17)$$

If the helicase perturbation is operational in a region between  $\phi = \phi_+$  to  $\phi = \phi_-$ , then the velocity can be written as

$$c = D \frac{\Delta F}{\mathcal{E}}, \quad (18)$$

where  $\mathcal{E} = \int [\phi'_0(z)]^2 dz$  is the kink energy and

$$\Delta F = \int_{\phi_-}^{\phi_+} \delta f(\phi) d\phi$$

is the free energy cost per unit length in the region of the bite. The expression for the kink energy follows from equations (13) and (8). The velocity found in equation (18) is positive, as it should be.

This procedure can be implemented for the RecG case, equation (10). The instability of the interface now leads to a moving front, but with a negative velocity, at least in the perturbative regime. The perturbation theory via the Goldstone mode yields

$$c = -h_R \frac{1}{\mathcal{E}} \left( \frac{\partial \phi_0}{\partial z} \right)^2 \Big|_{-}^{+}, \quad (19)$$

where the limits are the two end points of the bite. What we see is a negative velocity because of the reduction of the elastic constant and the curvature of the profile of the zeroth-order interface near  $\phi = 0$ . By symmetry one would get a positive velocity if the perturbation were at  $\phi = 1$ .

### 3.1. Numerical solution

The perturbation theory is around the static solution and need not be valid in practical situations. More structures can be expected if we look at the nonperturbative effects of the helicase term in the presence of the dynamically generated front. To do so, we solved the discretized versions of the equations numerically via an implicit procedure. The arbitrary lattice spacing  $\Delta z$  and time  $\Delta t$  are chosen small for convergence. We have taken  $\Delta t = 10^{-4}$  and  $\Delta z = 10^{-2}$ . All the other parameters are chosen in these units.

The results are shown in figures 4 and 5 in discretized  $z$  and time  $t$ . The location  $z_0$  of the interface is taken to be the point where  $\phi = 0.5$ . We start with a sharp interface at time  $t = 0$ , with  $z_0$  chosen away from the boundary. Initial transients allow the interface to evolve to its natural shape. This shape in the steady state has been found not to depend on the initial profile. The perturbations are applied over a region as indicated in figure 4. For figure 4(a), the local perturbation favours the unzipped state, as shown in figure 3(a) while in figure 4(b),  $h_R$  perturbation makes both states unstable (figure 3(b)). The velocity measurements were done once the steady state was reached and the interface is not close to the boundaries thus avoiding finite size or boundary effects.

A check on the perturbation theory would be the linearity of the velocity for small perturbations. We have verified this and also the fact that for a wide perturbation (much larger than the width of the interface) the velocity should saturate to the bulk value [15]. These verifications are not shown here. Figure 4 shows the change in the direction of the velocity by the two perturbations. In (a) the helicase bites at a particular value of  $\phi = 0.5$ , but since the perturbation makes the  $\phi = 0$  state metastable, the propagation is always towards the zipped side—opening of DNA. In case (b), the bite is also at a particular value of  $\phi$ , but close to the bound state side. We chose  $\phi = 0.1$ . Owing to the instability of the

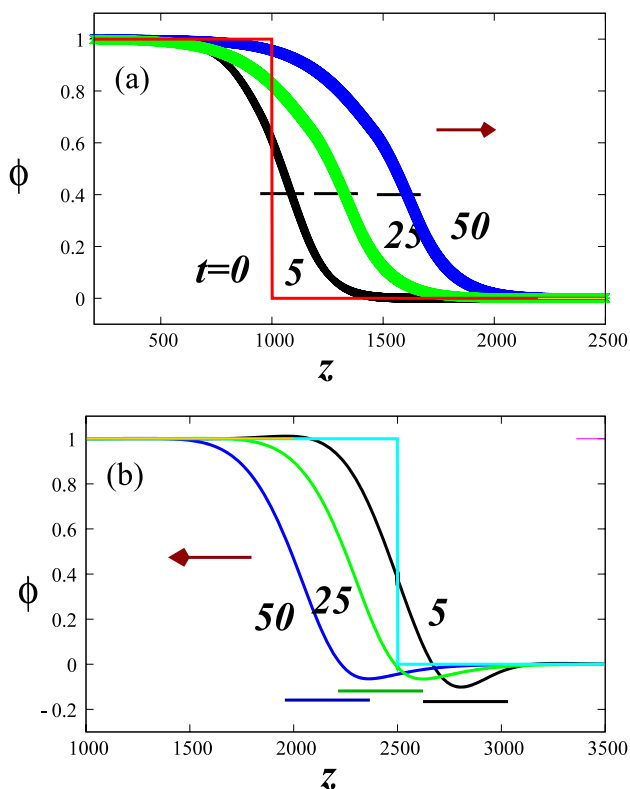


**Figure 4.**  $\phi$  versus  $z$  profile for various times as marked. Both  $z$  and  $t$  are discretized. (a) For a general helicase, equation (4) and (b) for a RecG type case for equation (10). The horizontal bar indicates the location of the perturbation. In (a) the helicase bites at  $\phi = 0.5$  while in (b) the bite is at  $\phi = 0.1$ , in both cases over a length  $2W$ . We see the velocity (direction indicated by an arrow) towards the zipped side in (a) but in the opposite direction in (b). The data are for  $D = \gamma = 1, h_R = 2$ , so that  $D' < 0$ .

profile, there is a push towards the unzipped side. The profile in figure 4(b) shows the structure developed—the monotonicity of the profile of figure 4(a) has gone. This non-monotonicity can lead to new phenomenon not captured by the first-order perturbation. Depending on the width of the bite, there may even be a cancellation in equation (19), as we see in the case marked 400 (ignoring the initial transients). In this situation, the helicase would have a stop-and-go type motion, of course towards the unzipped side. Though RecG may not do so, there are other helicases, such as RecQ and RecA, which are known to have such peculiar motions. Therefore the proposed destabilizing mechanism can lead to a variety of motions. Moreover, these parameters provide us with a set of values to classify or differentiate the helicases quantitatively.

#### 4. Summary

A few comments can be made here. In the case of forward propagation due to bulk instability, almost a century old problem [23], there is a push to pull type dynamic transition, as reflected in the nature of the velocity of propagation [24]. In our approach, the biochemically controllable width  $W$ , within which a helicase works, actually acts as a finite length cut-off for the bulk transition, and, therefore, it provides a new testing

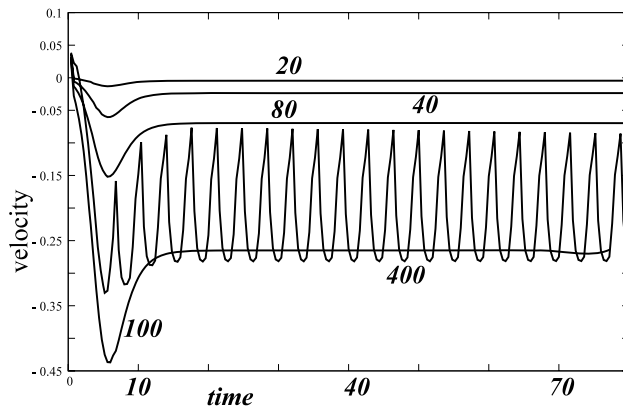


**Figure 5.** Velocity as a function of time for the RecG type case. As a result of the continuous change of the profile, the velocity may show a time dependence, as seen in the case marked 400 (the spatial width of the perturbation in arbitrary units). The same situation as in figure 4(b).

ground for any finite size scaling of the bulk nonequilibrium transition. This would be an extremely interesting situation where a biological problem can shed new lights on an age-old physics/material science problem.

Biological models have so far ignored the importance of the interface or of treating the Y-fork as a coexistence. We hope our results will motivate new experiments to measure the elastic energy of the interface ( $D$ ), possibly via an independent propagation velocity measurement. In addition, the helicases need to be classified by the nature of the perturbation and its strength and width. One needs to wait for these independent experimental results for any quantitative comparisons between the model calculations presented here and related biological experiments.

We summarize our results here. The Y-fork generated by a helicase, if kept in equilibrium, is a coexistence of two phases. Ordinary helicases work by destabilizing the zipped phase near the interface and the local instability leads to the Y-fork motion towards the zipped side, thereby opening the fork. For RecG, the aromatic interaction between the helicase and the interface leads to a destabilization of the interface, and this could close the DNA by a fork motion towards the open side. We show this by a perturbation method that also verifies the results for the ordinary case. A numerically exact solution is used to study the Y-fork motion in the presence of the dynamically generated front. In the interface destabilization case, more a complex stop-and-go type motion is found to be possible. Coming back to the problem of replication, our results enable us now to use this formulation to describe the replication in a co-moving frame with the Y-fork, bypassing a direct reference to the helicase. The next step is to couple the Y-fork motion with the polymerase activity.

#### References

- [1] Lehninger A L 2008 *Principles of Biochemistry* 5th edn (New York: Freeman)
- [2] Baker T A and Bell S P 1998 *Cell* **92** 295
- [3] Schrock R D and Alberts B 1996 *J. Biol. Chem.* **271** 16678

- [4] O'Donnell M 2006 *J. Biol. Chem.* **281** 10653  
Yao Nina Y *et al* 2009 *Proc. Natl Acad. Sci.* **106** 13236
- [5] Stano N M *et al* 2005 *Nature* **435** 370
- [6] Trakselis M A *et al* 2001 *Proc. Natl Acad. Sci.* **98** 8368
- [7] Lovett S T 2007 *Mol. Cell* **27** 523
- [8] Anderson S and DePamphilis M L 1979 *J. Biol. Chem.* **254** 11495  
Chastain P D II *et al* 2000 *Mol. Cell* **6** 803
- [9] Cowan R 2001 *Handbook of Statistics* vol 20, ed C R Rao and D N Shanbang (Amsterdam: North-Holland) p 137
- [10] Fass D, Bogden C E and Berger J M 1999 *Structure* **7** 691
- [11] Soultanas P *et al* 2000 *EMBO J.* **19** 3799
- [12] Atkinson J and McGlynn P 2009 *Nucleic Acids Res.* **37** 3475
- [13] Singleton M R, Scaife S and Wigley D B 2001 *Cell* **107** 79
- [14] Martinez-Senac M M and Webb M R 2005 *Biochemistry* **44** 16967
- [15] Bhattacharjee S M 2004 *Europhys. Lett.* **65** 574
- [16] Bhattacharjee S M 2000 *J. Phys. A: Math. Gen.* **33** L423 (arXiv:cond-mat/9912297)
- [17] Chen J Z Y 2002 *Phys. Rev. E* **66** 031912  
Allahverdyan A E *et al* 2004 *Phys. Rev. E* **69** 061908  
Lam P-M, Levy J C S and Huang H 2004 *Biopolymers* **73** 293  
Kapri R 2009 *J. Chem. Phys.* **130** 145105
- [18] Marenduzzo D, Trovato A and Maritan A 2001 *Phys. Rev. E* **64** 031901
- [19] Kapri R, Bhattacharjee S M and Seno F 2004 *Phys. Rev. Lett.* **93** 248102  
Kapri R and Bhattacharjee S M 2007 *Phys. Rev. Lett.* **98** 098101
- [20] Kumar S, Giri D and Singh Y 2005 *Europhys. Lett.* **70** 15  
Giri D and Kumar S 2006 *Phys. Rev. E* **73** 050903(R)
- [21] Cocco S, Monasson R and Marko J F 2002 *Phys. Rev. E* **66** 051914  
Kafri Y, Mukamel D and Peliti L 2002 *Eur. Phys. J. B* **27** 135
- [22] Bianco P R *et al* 2001 *Nature* **409** 374  
Dohoney K M and Gelles J 2001 *Nature* **409** 370
- [23] Luther R 1906 *Z. Elektrochem. Angew. Chem.* **12** 596  
Fisher R A 1937 *Ann. Eugenics.* **7** 355  
Kolmogorov A, Petrovsky L and Piscounoff N 1937 *Bull. Univ. Mosc.* **A 1** 1
- [24] van Saarloos W 2003 *Phys. Rep.* **386** 29  
Murray J D 2002 *Mathematical Biology: An Introduction* 3rd edn (New York: Springer)
- [25] Chaikin P M and Lubensky T C 1995 *Principles of Condensed Matter Physics* (Cambridge: Cambridge University Press)